Photoassociation intensities and radiative trap loss in lithium

R. Côté and A. Dalgarno
Harvard-Smithsonian Center for Astrophysics, 60 Garden Street, Cambridge, Massachusetts 02138
(Received 17 November 1997; revised manuscript received 17 February 1998)

We interpret measurements of photoassociative spectroscopy in a gas of lithium atoms at ultralow temperatures in which photons are absorbed into high vibrational levels of excited electronic singlet and triplet states of Li_2. The excited vibrational levels decay by spontaneous emission into the vibrational continuum and the discrete vibrational levels of the ground singlet and lowest triplet electronic states. Spontaneous emission into discrete levels produces molecules that are no longer trapped, and decay into the vibrational continuum can produce atoms with sufficient kinetic energy to escape the trap. We present values of the efficiencies of trap loss by radiative excitation as a function of the trap depth for individual excited vibrational levels of the singlet and triplet states of the $^6Li_2$ and $^7Li_2$ molecules.
[S1050-2947(98)06107-1]

PACS number(s): 32.80.Pj, 33.20.−t, 33.20.Tp, 33.50.Dq

I. INTRODUCTION

Recent advances in laser cooling and trapping, and in evaporative cooling techniques, have opened the possibility of studying new classes of physical systems at ultralow temperatures [1,2], as demonstrated by the realization of Bose-Einstein condensation of alkali-metal atoms [3–5]. Laser cooling techniques have played a key role in the photoassociation spectroscopy of gases of ultracold alkali-metal atoms [6–9], which has led to significant advances in the quantitative understanding of atomic interactions and processes.

The success of these experiments depends on the atom densities obtained in the traps, which are limited by escape mechanisms. We explore here one of the escape mechanisms, radiative escape (RE), which occurs by spontaneous emission of the vibrational levels populated in photoassociative spectroscopy.

In Sec. II, we review the theory of absorption of a photon into a discrete vibrational level of the excited electronic state from the vibrational continuum of the ground electronic state. We describe the interaction potentials and the dipole moments and comment on the resulting photoabsorption spectra. We give expressions for spontaneous and stimulated emission in Sec. III and discuss the decay of the excited vibrational levels into discrete and continuum vibrational levels of the ground electronic states. In Sec. IV, we evaluate the fraction of atoms recaptured by the trap after decay and calculate the efficiency of trap loss by radiative excitations as a function of the trap depth.

II. PHOTOABSORPTION THEORY

In the absorption of a photon by a pair of colliding atoms, the atoms make a transition from the vibrational continuum of the ground electronic state of the molecule to a bound vibrational level of an excited electronic state. The free-bound absorption rate coefficient at a laser frequency ν of a pair of atoms may be written [10]

$$\kappa(\nu,v)=\left\langle \frac{n^2\pi\hbar}{k}\sum_{v'}\sum_{J=0}^{\infty}(2J+1)|S_{v'}(E,J,\nu)|^2\right\rangle, \quad (1)$$

where E is the kinetic energy, v' is the vibrational quantum number of the excited state, J is the angular momentum quantum number of the initial state, $S_{v'}(E,J,\nu)$ is the free-bound transition amplitude, n is the gas density, and $\langle\ \rangle$ is an average over the distribution of initial velocities $\hbar k$ [10]. If a Maxwellian distribution at temperature T is assumed, expression (1) yields for the absorption coefficient

$$\kappa(\nu,T)=\sum_{v'}\sum_{J=0}^{\infty}(2J+1)\frac{n^2}{hQ_T}\int_0^{\infty}dEe^{-E/kT}|S_{v'}(E,J,\nu)|^2, \quad (2)$$

where $Q_T=(2\pi\mu k_BT/h^2)^{3/2}$ and μ is the reduced mass. The square of the S-matrix element $|S_{v'}(E,J,\nu)|^2$ can be approximated by $\gamma_{v'}\gamma_s(E,J)/[(E-\Delta_{v'})^2+(\gamma/2)^2]$, where $\Delta_{v'}=E_{v'}-h\nu$ is the detuning relative to position $E_{v'}$ of the bound level v' [10]. The width of level v' is given by $\gamma(v')=\gamma_{v'}+\gamma_s(E,J)+\gamma_0$, where $\gamma_{v'}/\hbar$ is the rate of spontaneous decay of the bound state, $\gamma_s(E,J)/\hbar$ is the stimulated emission rate back to the ground state, and $\gamma_0/\hbar$ is the decay rate due to any other undetected processes such as molecular predissociation; γ_0 is presumed negligible here.

At low laser intensities, the stimulated decay rate is proportional to the laser intensity I and, for the transition from an initial bound state with nuclear wave function $u_{v'J'}$ to a final continuum state with nuclear wave function $u_{E,J}$, is given by

$$\gamma_s(E,J)=4\pi^2\frac{I}{c}|\langle u_{E,J}|D(R)|u_{v',J'}\rangle|^2, \quad (3)$$

where $D(R)$ is the electronic transition moment connecting the initial and final electronic states. For a Σ-Σ molecular transition, $J=J'\pm1$. When I is small, the form of $S_{v'}(E,J,\nu)$ simplifies to

$$|S_{v'}(E,J,\nu)|^2=2\pi\gamma_s(E,J)\,\delta(E-\Delta_{v'}). \quad (4)$$

Dividing by the incident photon flux $Ic/8\pi h\nu$, we get the absorption rate coefficient [11]

TABLE I. Statistical weights for the two lithium isotopes. $S=0$ is the singlet and $S=1$ the triplet.

S	^{6}Li ($I=1$) ω_J		^{7}Li ($I=\frac{3}{2}$) ω_J	
	J odd	J even	J odd	J even
0	$\frac{1}{12}$	$\frac{1}{6}$	$\frac{5}{32}$	$\frac{3}{32}$
1	$\frac{1}{2}$	$\frac{1}{4}$	$\frac{9}{32}$	$\frac{15}{32}$

$$\kappa(\nu,T)=\frac{8\pi^3\nu}{3c}\frac{n^2}{Q_T}\sum_{v'}\exp(-E/k_BT)\times\sum_J\omega_J[(J+1)|\langle u_{v',J+1}|D|u_{E,J}\rangle|^2+J|\langle u_{v',J-1}|D|u_{E,J}\rangle|^2], \quad (5)$$

where $E=\Delta_{v'}$, and ω_J are statistical weights that depend on the hyperfine states of the interacting atoms and on the nuclear spin [12]. They are listed in Table I for a statistical distribution of hyperfine states of isotopes ^{7}Li and ^{6}Li.

In the Born-Oppenheimer approximation, the radial wave function of the excited bound state $u_{v',J'}(R)$ is the well-behaved normalized solution of the equation

$$\left(\frac{d^2}{dR^2}+\frac{2\mu}{\hbar^2}E_{v',J'}-\frac{2\mu}{\hbar^2}V_x(R)-\frac{J'(J'+1)}{R^2}\right)u_{v',J'}(R)=0, \quad (6)$$

where $E_{v',J'}$ is the eigenvalue and $V_x(R)$ is the excited interatomic potential.

The initial free ground-state eigenfunction $u_{E,J}(R)$ is the regular solution of the partial wave equation

$$\left(\frac{d^2}{dR^2}+k^2-\frac{2\mu}{\hbar^2}V_g(R)-\frac{J(J+1)}{R^2}\right)u_{E,J}(R)=0, \quad (7)$$

where $V_g(R)$ is the ground-state interatomic potential, and $E=\hbar^2k^2/2\mu$. The radial wave function is normalized with respect to the energy, and $u_{E,J}(R)$ has the asymptotic form

$$u_{E,J}(R)\sim\left(\frac{2\mu}{\pi\hbar^2k}\right)^{1/2}\sin\left[kR-\frac{J\pi}{2}+\delta_J(k)\right], \quad (8)$$

where $\delta_J(k)$ is the elastic scattering phase shift.

The two possible states formed by the approach of the two Li ($2s$) atoms are the singlet $X^1\Sigma_g^+$ and triplet $a^3\Sigma_u^+$ states. We consider photons detuned more than 20 GHz to the red from the degeneracy-weighted average of the $2s$-$2p$ resonance lines. The region closer than 20 GHz is not included here because of complications of spin-orbit and hyperfine splittings with spin no longer a good quantum number. States with potential curves lying below the Li($2s$)+Li($2p$) separated atom limit are candidates for absorption. For the singlet transitions, the sole possibility at large distances is the $X^1\Sigma_g^+\rightarrow A^1\Sigma_u^+$ transition [at short distances the $B^1\Pi_u$ potential curve also lies below the Li($2s$)+Li($2p$) asymptote]. For triplet transitions, the $a^3\Sigma_u^+\rightarrow 1^3\Sigma_g^+$ transition is the sole possibility.

For the two lower state potentials we adopt those described in [13]. It is assumed here that the potential energy curves of $^6Li_2$ and $^7Li_2$ are identical, although there is evidence for small dissociation energy differences (~ 0.5 cm^{-1}) [14,15]. To construct the two excited state potentials, we used RKR data supplemented by *ab initio* values. For the $A^1\Sigma_u^+$ state we used the RKR data from Kusch and Hessel [16] between $R=4.13a_0$ and $R=10.21a_0$. *Ab initio* data from Schmidt-Mink, Müller, and Meyer [17] were used between $R=3.25$ and $4.00a_0$ and between $R=10.5$ and $30.0a_0$. In the case of the $1^3\Sigma_g^+$ state, we used RKR data from Linton *et al.* [18] between $R=4.66a_0$ and $R=7.84a_0$ and we extended them with *ab initio* values from Schmidt-Mink *et al.* [17] for distances between $R=3.25$ and $4.50a_0$ and between $R=8.00$ and $30.0a_0$. Because the *ab initio* data extended to large distances, we did not need an explicit representation of the exchange terms, which are included in the *ab initio* calculations. For both excited curves, we extended the potentials to large distances with the long range form of the potential

$$V(R)\simeq-\frac{C_3}{R^3}-\frac{C_6}{R^6}-\frac{C_8}{R^8}. \quad (9)$$

We used $C_3=11.01$, $C_6=2066$, and $C_8=270\,500$ from Marinescu and Dalgarno [19] expressed in atomic units. More precise values of the long range coefficients [20], more accurate lower state potentials [22], and new and and more extensive RKR results for the $A^1\Sigma_u^+$ state of $^6Li_2$ [15] and of $^7Li_2$ [23] became available after our calculations were completed. These modifications would cause only slight differences in our results [21].

We used the values $D_{\rm RFK}$ of the electronic transition moment $D(R)$ calculated by Ratcliff, Fish, and Konowalow [24] for distances ranging from 3.5 to $35.0a_0$ for the singlet and triplet transitions, rescaled by a factor f_S to match the asymptotic form (in a.u.)

$$D(R)\simeq D_0+\frac{b}{R^3}, \quad (10)$$

with $D_0=3.3175$ and $b=283.07$ derived by Marinescu and Dalgarno [19]. We define f_S by $(D_0+b/35.0^3)/D_{\rm RFK}(35.0)$, and for $R<35.0a_0$ we write $D(R)=f_SD_{\rm RFK}(R)$. For $R<3.5a_0$ we use the linear form $D(R)=D(3.5)+(R-3.5)dD(R)/dR|_{3.5}$.

III. RESULTS

At ultralow temperatures, only the s-wave ($J=0$) collisions penetrate into the short internuclear distances where significantly detuned (>20 GHz) absorption occurs. Using the expression (5) with $J=0$, we computed the lithium photoabsorption coefficient

$$\kappa(\nu,T) \simeq \frac{8\pi^3\nu}{3c}\frac{n^2}{Q_T}\sum_{v'}\omega_0 \exp(-E/k_BT)|\langle u_{v',1}|D|u_{E,0}\rangle|^2, \tag{11}$$

where $\omega_{J=0}$ is given in Table I. The absolute values of $\kappa(\nu,T)$ for $T=1$ mK are given in Table II for excited levels $v' \geqslant 51$ of the singlet and triplet states of $^7Li_2$ and $^6Li_2$ in units of cm^5, except that levels of high v' for which the detuning is less than 20 GHz are excluded since they are significantly affected by spin-orbit and hyperfine interactions. A semiclassical estimate of a quantity related to $\kappa(\nu,T)$ has been given by Pillet *et al.* [25] but not for specific vibrational levels. Figure 1 illustrates the absorption rate coefficients for ^{7}Li and ^{6}Li at frequency intervals Δ between 0 and 1000 GHz offset from the resonance line. The detuning Δ is related to the energy E and the frequency ν through $h\nu = E_{v'} - E = \hbar\omega_p + \hbar\Delta$, where $\hbar\omega_p$ is the energy difference between the dissociation limits of the excited and ground states and $E_{v'}$ is the energy of the bound state v' relative to the dissociation limit of the initial state of Li_2.

For each isotope, there occurs two series of absorptions, one strong and one weak. The stronger one originates from the triplet transition $a^3\Sigma_u^+ \rightarrow 1^3\Sigma_g^+$ and persists to large values of the detuning [9]. The weaker series is due to the singlet transition $X^1\Sigma_g^+ \rightarrow A^1\Sigma_u^+$ and it becomes negligible at detunings greater than 200 GHz [9].

The triplet photoabsorption lines have been observed down to -2249 GHz, corresponding to vibrational level $v' = 62$ for ^{7}Li and -2706 GHz corresponding to $v' = 56$ for ^{6}Li [9]. In the case of the singlet transitions, the lines have negligible strength for Δ below -400 GHz for ^{7}Li and -200 GHz for ^{6}Li, corresponding to $v' = 82$ and 79, respectively. More precise measurements on singlet transitions [26] were made for levels down to $v' = 62$ and 65 for ^{6}Li and ^{7}Li, respectively.

Some of the difference in intensities between the singlet and triplet series comes from the statistical weights, which for the singlet and triplet states have $\omega_0 = 3/32$ and 15/32, respectively, for ^{7}Li and $\omega_0 = 1/6$ and 1/4, respectively, for ^{6}Li. The remaining differences and the disappearance of the singlet signal at higher detunings arise from the behavior of dipole moment integrals and depend on the scattering length [27]. We show in Figs. 2 and 3 the square of the dipole matrix element

$$|D_{v'}(E)|^2 \equiv |\langle u_{v',J'=1}|D|u_{E,J=0}\rangle|^2, \tag{12}$$

for ten vibrational levels v' as a function of the initial energy E for the singlet and triplet transitions. The values of $|D_v(E)|^2$ maximize at a value of E near to a temperature of 10 mK. As we will show in Sec. IV, this implies that the sequence of absorption and emission is a heating mechanism in a trap maintained at 1 mK.

The triplet strengths in Fig. 3 are much larger than the singlet strengths in Fig. 2. The bound level wave functions corresponding to $v' = 89$ and $\Delta = -107$ GHz for the singlet state and $v' = 80$ and $\Delta = -120$ GHz for the triplet state are reproduced in Fig. 4. Both are rapidly oscillating functions with small amplitudes, until the last lobe centered around $80-83a_0$ is reached.

TABLE II. Photoabsorption rate coefficients $\kappa_{v'}$ for unit densities at $T=1$ mK for high excited levels v' (in cm^5). The dashes indicate levels for which spin-orbit coupling becomes important, corresponding to detunings smaller than 20 GHz. Brackets represent powers of ten.

	triplet		singlet	
v'	^{6}Li	^{7}Li	^{6}Li	^{7}Li
51	2.38 [−35]	2.46 [−37]	1.64 [−37]	9.94 [−38]
52	1.25 [−35]	7.23 [−37]	3.25 [−37]	7.86 [−38]
53	2.46 [−36]	1.35 [−36]	4.92 [−37]	1.83 [−38]
54	1.17 [−36]	1.98 [−36]	4.52 [−37]	2.23 [−39]
55	1.84 [−35]	2.48 [−36]	3.53 [−37]	6.23 [−38]
56	5.67 [−35]	2.71 [−36]	1.50 [−37]	1.84 [−37]
57	1.05 [−34]	2.57 [−36]	3.22 [−38]	2.91 [−37]
58	1.62 [−34]	2.00 [−36]	1.66 [−38]	3.39 [−37]
59	2.29 [−34]	1.10 [−36]	1.81 [−37]	2.68 [−37]
60	3.11 [−34]	2.62 [−37]	6.42 [−37]	1.65 [−37]
61	4.17 [−34]	1.08 [−38]	1.33 [−36]	4.79 [−38]
62	5.60 [−34]	4.89 [−37]	2.41 [−36]	3.77 [−40]
63	7.25 [−34]	1.63 [−36]	3.41 [−36]	5.74 [−38]
64	8.75 [−34]	3.51 [−36]	4.08 [−36]	2.41 [−37]
65	1.05 [−33]	6.30 [−36]	4.07 [−36]	6.15 [−37]
66	1.25 [−33]	1.04 [−35]	4.07 [−36]	1.10 [−36]
67	1.46 [−33]	1.66 [−35]	3.86 [−36]	1.75 [−36]
68	1.71 [−33]	2.48 [−35]	3.66 [−36]	2.26 [−36]
69	1.98 [−33]	3.41 [−35]	3.29 [−36]	2.48 [−36]
70	2.29 [−33]	4.58 [−35]	2.90 [−36]	2.27 [−36]
71	2.65 [−33]	6.03 [−35]	2.14 [−36]	2.04 [−36]
72	3.06 [−33]	7.78 [−35]	1.29 [−36]	1.73 [−36]
73	3.54 [−33]	9.91 [−35]	5.33 [−37]	1.41 [−36]
74	4.11 [−33]	1.25 [−34]	7.25 [−38]	1.03 [−36]
75	4.79 [−33]	1.57 [−34]	9.79 [−38]	6.83 [−37]
76	5.61 [−33]	1.96 [−34]	9.60 [−37]	3.04 [−37]
77	6.61 [−33]	2.45 [−34]	3.19 [−36]	4.33 [−38]
78	7.86 [−33]	3.05 [−34]	7.43 [−36]	4.60 [−38]
79	9.41 [−33]	3.82 [−34]	1.48 [−35]	4.54 [−37]
80	1.14 [−32]	4.78 [−34]	2.68 [−35]	1.49 [−36]
81	–	6.02 [−34]	4.58 [−35]	3.35 [−36]
82	–	7.62 [−34]	7.50 [−35]	6.46 [−36]
83	–	9.70 [−34]	1.20 [−34]	1.12 [−35]
84	–	1.24 [−33]	1.87 [−34]	1.83 [−35]
85	–	1.61 [−33]	2.90 [−34]	2.85 [−35]
86		2.10 [−33]	4.45 [−34]	4.32 [−35]
87		–	6.81 [−34]	6.40 [−35]
88		–	1.04 [−33]	9.35 [−35]
89		–	–	1.35 [−34]
90		–	–	1.93 [−34]
91		–	–	2.76 [−34]
92			–	3.94 [−34]
93				5.60 [−34]
94				8.00 [−34]
95				1.15 [−33]
96				–
97				–
98				–
99				–
100				–

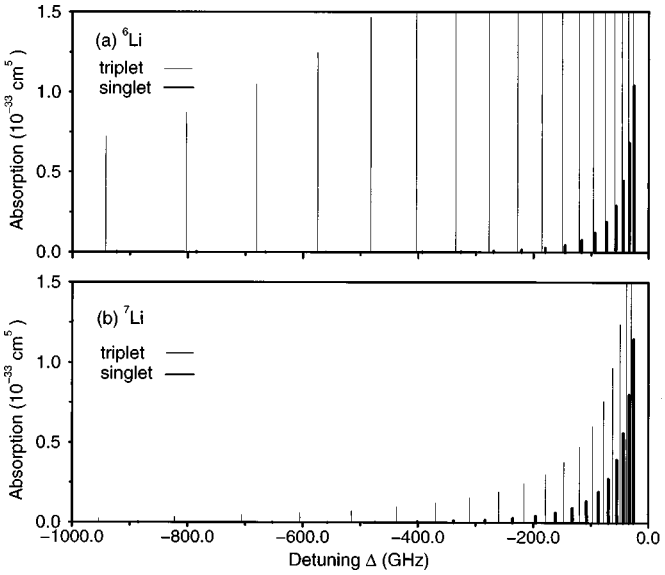

FIG. 1. Theoretical photoabsorption coefficients in units of 10^{-33} cm^5 as a function of the detuning (GHz) for (a) ^{6}Li and (b) ^{7}Li.

Most of the contribution to the integral $D_{v'}(E)$ comes from the overlap of this last lobe with the product of the free wave function and the dipole moment. Since $D(R)$ varies slowly for large R, $D(R)$ can be taken as a constant D_0 for both singlet and triplet transitions, and we may write

$$|D_{v'}(E)|^2=\left|\int_0^\infty dR u_{v',J'=1}(R)D(R)u_{E,J=0}(R)\right|^2$$
$$\simeq\left|\int_{R_1}^{R_2} dR u_{v',1}(R)D(R)u_{E,0}(R)\right|^2$$
$$\simeq|D_0|^2\left|\int_{R_1}^{R_2} dR u_{v',1}(R)u_{E,0}(R)\right|^2, \qquad (13)$$

where R_1 and R_2 define the last lobe. As $E\to 0$, the free wave function takes, in the vicinity of the lobe, its asymptotic form

$$u_{E,0}(R)\simeq\left(\frac{2\mu}{\pi\hbar^2 k}\right)^{1/2}\sin\,\delta_0(k)\,\frac{\sin[kR+\delta_0(k)]}{\sin\,\delta_0(k)}$$
$$\simeq\left(\frac{2\mu}{\pi\hbar^2 k}\right)^{1/2}\sin\,\delta_0(k)[1+kR\,\cot\,\delta_0(k)]$$
$$\simeq\left(\frac{2\mu}{\pi\hbar^2 k}\right)^{1/2}\left(1-\frac{R}{a}\right)\sin\,\delta_0(k), \qquad (14)$$

where we used the effective range expansion

$$k\,\cot\,\delta_0(k)=-\frac{1}{a}+\frac{1}{2}r_e k^2+\cdots. \qquad (15)$$

In Eq. (15), a is the scattering length and r_e is the effective range. By the mean value theorem, we get

$$|D_{v'}(E)|^2\simeq|D_0|^2\left(\frac{2\mu}{\pi\hbar^2 k}\right)\sin^2\delta_0(k)$$
$$\times\left|\int_{R_1}^{R_2} dR\left(1-\frac{R}{a}\right)u_{v',1}(R)\right|^2$$
$$\simeq|D_0|^2\left(\frac{2\mu}{\pi\hbar^2 k}\right)\left(1-\frac{\overline{R}_{v'}}{a}\right)^2$$
$$\times L_{v'}^2|u_{v',1}(\overline{R}_{v'})|^2\sin^2\delta_0(k), \qquad (16)$$

where $\overline{R}_{v'}$ is the position of the center of the last lobe of level v' and $L_{v'}$ is the dimension of the lobe. $\overline{R}_{v'}$ corresponds to the classical outer turning point of the level v'. From the effective range expansion, we have

$$\sin^2\delta_0(k)=\frac{k^2}{k^2+k^2\,\cot^2\,\delta_0(k)}$$
$$\simeq a^2k^2[1+ak^2(r_e-a)]+\cdots, \qquad (17)$$

valid for energies up to $10^{-9}-10^{-8}$ a.u. in the case of $J=0$ [13]. Then, we have for $|D_{v'}(E)|^2$ the approximation

$$|D_{v'}(E)|^2\simeq\left(\frac{2\mu k}{\pi\hbar^2}\right)|D_0|^2(a-\overline{R}_v)^2L_{v'}^2|u_{v',1}(\overline{R}_{v'})|^2. \qquad (18)$$

Figure 4 illustrates the wave functions in the overlap region for the singlet $v'_S=89$ and triplet $v'_T=80$ bound levels, together with the free wave functions.

Equation (18) shows that the magnitude of $|D_{v'}(E)|^2$ is simply related to the scattering length a. For two adjacent peaks, like $v'_S=89$ and $v'_T=80$, the positions and dimensions of the last lobes of the bound-state wave functions are similar, and the difference in amplitude arises from the difference in the values of the scattering lengths. Since the scattering length for the triplet is negative [28,22], $|D^T_{v'}(E)|^2$ is always bigger than $|D^S_{v'}(E)|^2$ for neighboring higher vibrational levels.

This approximate expression for $|D_{v'}(E)|^2$ is valid in the low-energy limit but it applies well beyond $E\simeq 10^{-9}$ a.u. For the two high-lying levels considered earlier (see Fig. 4), the free wave functions have the same qualitative behavior for energies up to $E\simeq 10^{-8}$ a.u. corresponding to a temperature of 3.2 mK. Figure 5 illustrates the range of validity of Eq. (18) for the two levels selected here. The approximation gives good results up to $E=10^{-9}$ a.u. for $v'_T=80$ and 10^{-8} for $v'_S=89$.

As the vibrational level is lowered by increasing the detuning, a different behavior occurs for the singlet and the triplet signals. Because lowering v' decreases $\overline{R}_{v'}$, the singlet absorption decreases faster than the triplet, due to the difference in the sign of their scattering lengths and the singlet strengths pass through a zero at a value of $\overline{R}_{v'}$ near a_S, while the triplet absorptions do not.

The photoassociative spectrum is sensitive to the value of a in the case of a positive scattering length. Figure 6 shows

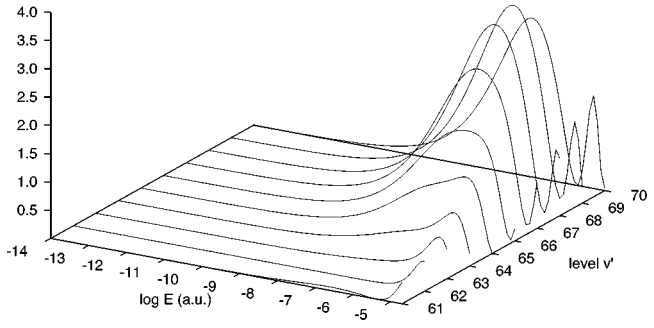

FIG. 2. Sequence of the dipole matrix element $|D_{v'}(E)|^2$ for ^{7}Li singlet transitions as a function of the kinetic energy (on a base 10 logarithmic scale) for various excited vibrational levels v. All quantities are in atomic units and $|D_{v'}(E)|^2$ must be multiplied by 10^5.

that a small variation of the dissociation energy of the ground-state potential translates into a large change of the scattering length. The resulting shift of the local dip in the spectrum is clearly identifiable. This sensitive signature can be used to infer a reliable value of the scattering length from experimental spectra. This method has been utilized in recent experiments [22] to derive singlet scattering lengths of $45.5 \pm 2.5 a_0$ for ^{6}Li and $33 \pm 2 a_0$ for ^{7}Li.

IV. SPONTANEOUS EMISSION

Trap loss occurs though the decay by spontaneous emission of the excited vibrational levels into the discrete and continuum vibrational electronic ground state. For the *R branch* with $J''=J'+1$, the spontaneous transition probability for a transition from vibrational level v' to vibrational level v'' is given by

$$A_{v'v''}=\frac{4}{3}\frac{e^2\omega_{v''v'}^3}{\hbar c^3}\frac{(J'+1)}{(2J'+1)}|\langle v''J''|D|v'J'\rangle|^2, \quad (19)$$

where $\omega_{v''v'}=(E_{v'',J''}-E_{v',J'})/\hbar$ is the frequency of the emitted photon. For the *P branch* with $J''=J'-1$, it is given by

$$A_{v'v''}=\frac{4}{3}\frac{e^2\omega_{v''v'}^3}{\hbar c^3}\frac{J'}{(2J'+1)}|\langle v''J''|D|v'J'\rangle|^2. \quad (20)$$

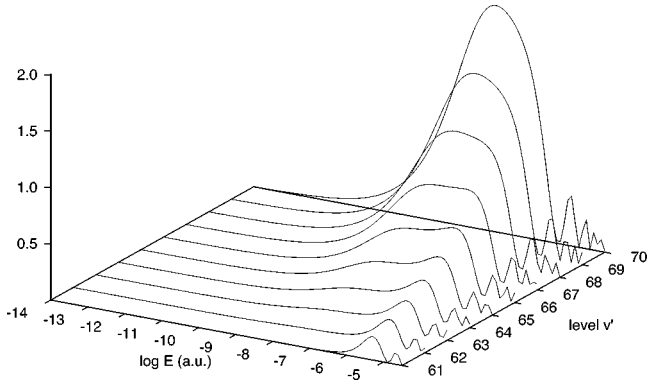

FIG. 3. As Fig. 2 for ^{7}Li triplet transitions. Here $|D_{v'}(E)|^2$ must be multiplied by 10^6.

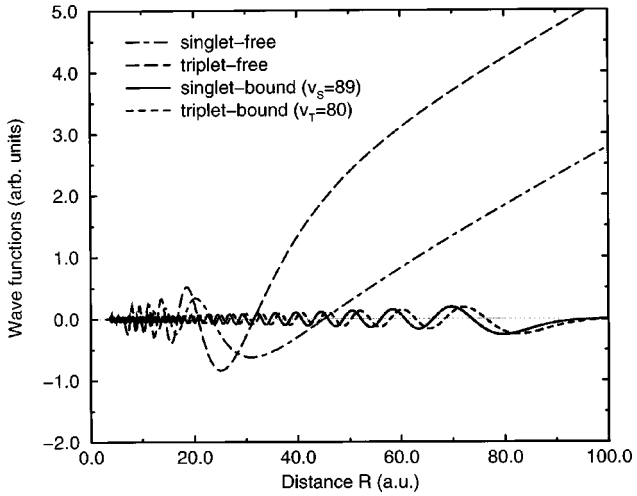

FIG. 4. Discrete wave functions for $v'_S=89$ of the singlet state and $v'_T=80$ for the triplet state of $^7Li_2$, and the singlet and triplet free wave functions at $E=10^{-12}$ a.u.

If we ignore centrifugal distortion we may write

$$A_{v'v''}=\frac{4}{3}\frac{e^2\omega_{v''v'}^3}{\hbar c^3}|\langle v''|D|v'\rangle|^2. \quad (21)$$

Spontaneous emission also occurs into the vibrational continuum of the lower state with probabilities $A_{v'}(\varepsilon'')$, where ε'' is the nuclear kinetic energy. The total transition probability for the spontaneous radiative decay of level v' is given by

$$A_{v'}=\sum_{v''} A_{v'v''}+\int d\varepsilon'' A_{v'}(\varepsilon''), \quad (22)$$

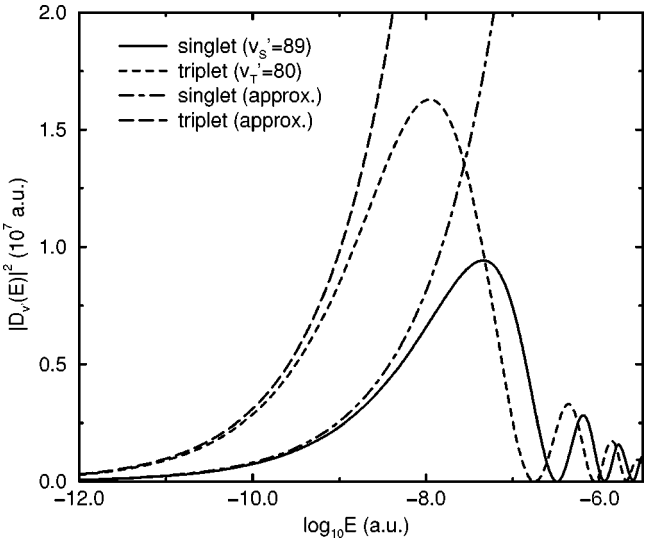

FIG. 5. Dipole matrix element $|D_{v'}(E)|^2$ for the excited singlet level $v'_S=89$ and triplet level $v'_T=80$ of $^7Li_2$. The approximate curves are computed using Eq. (18); for $v'_S=89$, $L=11, \overline{R}=83, u(\overline{R})=0.250$ and for $v'_T=80$, $L=10, \overline{R}=80, u(\overline{R})=0.255$. All quantities are in atomic units.

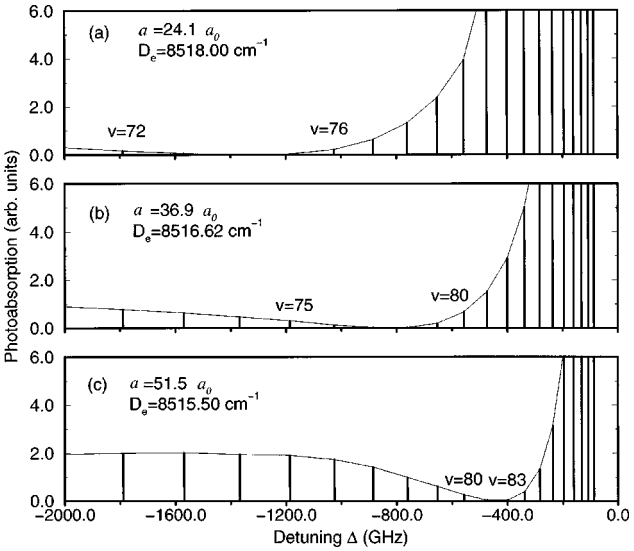

FIG. 6. Photoabsorption strengths for the singlet transitions of ^{7}Li for different values of the dissociation energy D_e and corresponding scattering length a. As the potential is deepened, the last bound level of the ground-state potential becomes more bound and the scattering length decreases.

where $A_{v'}(\varepsilon'')=\frac{4}{3}(e^2\omega_{v'}^3/\hbar c^3)|\langle\varepsilon''|D|v'\rangle|^2$ with $\omega_{v'}=(\varepsilon''-E_{v',J'=1})/\hbar$.

To estimate the contribution of the continuum states to $A_{v'}$, we assume that the relative transition probabilities are approximately equal to the Franck-Condon factors $q_{v'v''}=|\langle v'|v''\rangle|^2$. Then

$$A_{v'}\simeq\frac{\sum_{v''}A_{v'v''}}{\sum_{v''}q_{v'v''}},\tag{23}$$

where the sums are over the discrete levels only. To a similar approximation, the fraction of transitions that terminate in the continuum is given by $1-\Sigma_{v''}q_{v'v''}$.

In Fig. 7, we show $A_{v'}$ for the two isotopes, for v' up to 70 for the triplet transitions and to 80 for the singlet. For the singlet transitions $A_{v'}$ decreases slowly from 5.5×10^7 s^{-1} at $v'=0$ to 5.2×10^7 s^{-1} at $v'=20$ before growing steadily to its asymptotic value of 7.5×10^7 s^{-1}. For the triplet transitions, $A_{v'}$ increases monotonically from 2×10^7 s^{-1} to its asymptotic value of 7.35×10^7 s^{-1}. The correct value for both at large v' is 7.35×10^7 s^{-1}, any discrepancies arising from our approximate treatment of the continuum contributions.

To confirm this conclusion, we carried out an explicit evaluation of the continuum contributions for the $v'=80$ level of the triplet state and the $v'=88$ level of the singlet state of $^7Li_2$. The results are summarized in Table III. The levels decay preferentially into the continuum of the lower states. The radiative lifetimes $\tau_{v'}=A_{v'}^{-1}$ are nearly equal to the limiting value of 13.6 ns at infinite nuclear separation, which is half the atomic $2p$ lifetime. At large distances there are two pairs of Σ states separating to the $2s$-$2p$ limit, the $1^3\Sigma_g^+$ and $2^3\Sigma_u^+$ states and the $A^1\Sigma_u^+$ and $2^1\Sigma_g^+$ states. Transitions from the lower states to the $2^3\Sigma_u^+$ and $2^1\Sigma_g^+$ excited states are not allowed, and consequently the widths are zero. Since the atomic limit is equally made of two Σ states, it is the average of the molecular rates that tends to the atomic rate. The value of the atomic lifetime we obtain agrees well with the experimental value of 27.102 ns [29].

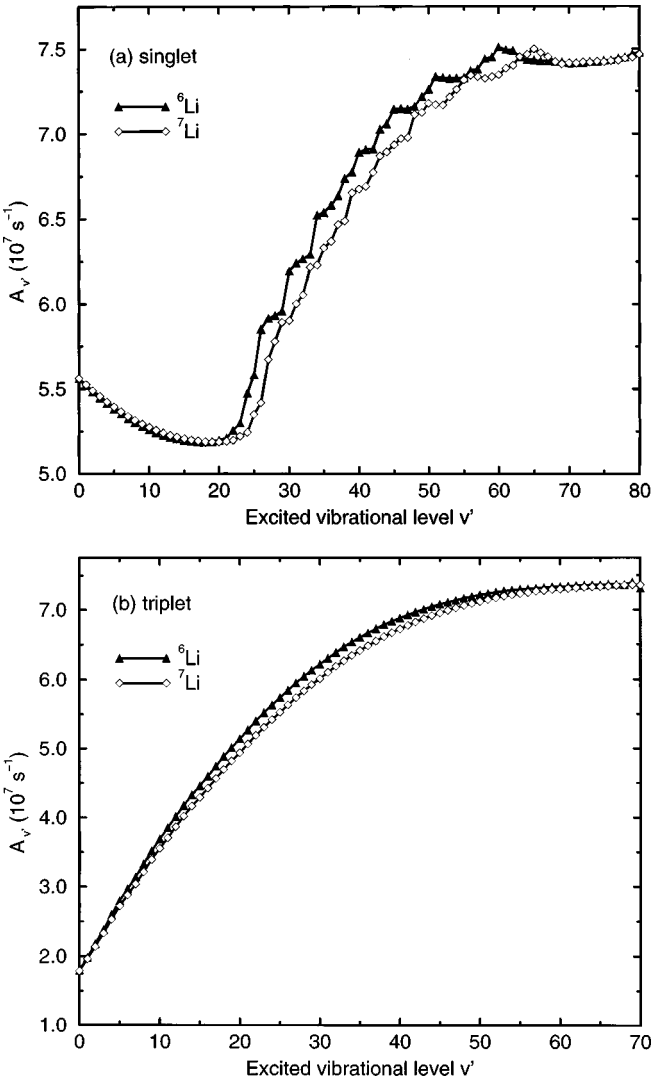

FIG. 7. Estimated $A_{v'}$ (in s^{-1}) of ^{6}Li and ^{7}Li for a given excited vibrational level v', (a) for singlet and (b) for triplet.

As mentioned in Sec. III, the sequence of absorption and emission is a heating mechanism in a trap maintained at 1 mK. To illustrate this more explicitly, we computed the spontaneous emission probabilities for the level $v'_T=60$ of the $1^3\Sigma_g^+$ state with $J'=1$, which decays into the continuum of the $a^3\Sigma_u^+$ state *via* spontaneous emission with $J''=0$ (*P branch*) or $J''=2$ (*R branch*). The kinetic energy distribution of a pair of atoms decaying into the continuum may be written

$$w_{v'}(J'\to J'',E)=A_{v'}(J'\to J'',E)\Big/\int_0^\infty dE'A_{v'}(J'\to J'',E'),\tag{24}$$

which insures that $\int_0^\infty dEw_{v'}(J'\to J'',E)=1$. The results are

TABLE III. Radiative transition probabilities and lifetimes for two excited levels of ^{7}Li. The experimental value for the atomic lifetime τ_{at} is 27.102 ns [29].

level	$\Sigma_{v''}A_{v'v''}$ (s^{-1})	$\int d\varepsilon'' A_{v'}(\varepsilon'')$ (s^{-1})	$A_{v'}$ (s^{-1})	$\tau_{v'}$ (ns)	τ_{at} (ns)
$v'_T=80$	3.47	7.344×10^7	7.344×10^7	13.617	27.233
$v'_S=88$	1.31×10^5	7.341×10^7	7.354×10^7	13.598	27.196

shown in Fig. 8. Although the *P branch* $(1\rightarrow0)$ distribution extends further to low energies than the *R branch* $(1\rightarrow2)$ distribution, $w_{v'}(J'\rightarrow J'',E)$ takes on small values for $E<10^{-6.5}$ a.u. (or $T<100$ mK) for both branches. It is clear that for both branches w peaks at energies corresponding to higher temperatures than 1 mK. Figure 8(a) shows that as E grows, w reaches a first maximum of 0.14 for the *P branch* and 0.16 for the *R branch* located at $E\sim10^{-5.0}$ a.u. (or $T\sim3$ K), followed by many oscillations with increasing magnitudes up to 0.4 at $E\sim10^{-3.8}$ a.u. and then decreasing magnitudes for higher energies. In Fig. 8(b), we show the integrated value of w as a function of E, namely $W_{v'}(J'\rightarrow J'',E)\equiv\int_0^E dE' w_{v'}(J'\rightarrow J'',E')$. Fewer than 1% of the pairs of atoms decay with energies smaller than $10^{-5.5}$ a.u. (or $T\sim1$ K) for the *P branch*, and fewer than 0.3% for the *R branch*. Only 10% of the pairs acquire kinetic energy less than $10^{-5.0}$ a.u. ($T\sim3$ K) after spontaneous emission for both branches. So indeed, most pairs of atoms are heated by the process.

Finally, to illustrate that the effect of centrifugal distortion is small, we computed $\gamma_{v'}(J'\rightarrow J'')\equiv\int_0^\infty dE A_{v'}(J'\rightarrow J'',E)$ without the $J'/(2J'+1)$ and $(J'+1)/(2J'+1)$ factors. We obtained $\gamma=6.41\times10^7$ s^{-1} for the *P branch* $(1\rightarrow0)$ and $\gamma=6.36\times10^7$ s^{-1} for the *R branch* $(1\rightarrow2)$, showing a centrifugal distortion effect less than 0.8%.

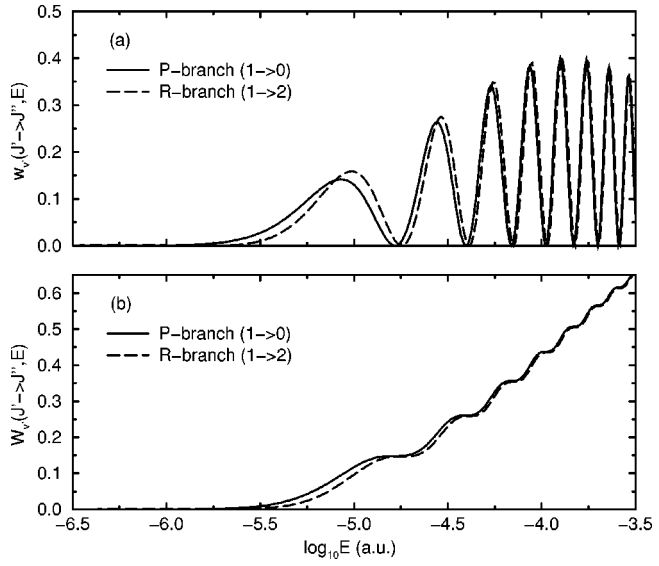

FIG. 8. Kinetic energy distribution for a pair of atoms undergoing spontaneous decay from the level $v'_T=60$ of the excited triplet state $1^3\Sigma_g^+$ of $^7Li_2$ with $J'=1$. In (a) we show the distribution $w_{v'}(J'\rightarrow J'',E)$ for the *P* and *R branches*, and in (b) the integrated distribution $W_{v'}(J'\rightarrow J'',E)$.

V. TRAP LOSS

In a magneto-optical trap (MOT), many different processes can lead to trap loss. Spin-flip during the collision can transfer large amounts of energy to the motion of the atoms allowing them to escape and dipole relaxation can accomplish a similar effect. Two collisional loss mechanisms involving excited and ground-state ultracold atoms have been identified [30]. The first mechanism, a fine-structure-changing collision (FS), occurs when the colliding atom pair is excited to a molecular potential correlating with $S_{1/2}+P_{3/2}$ atomic state and exits on a molecular potential correlating with the $S_{1/2}+P_{1/2}$ atomic states. The difference in energy E_{FS} between the fine-structure levels is divided between the atom pair as kinetic energy. If the trap depth E_T is less than $\frac{1}{2}E_{FS}$, the pair is ejected from the trap. In the case of lithium, since E_{FS} ($E_{FS}/k_B=0.48$ K) is comparable to E_T in a MOT, FS can be suppressed by insuring that $E_T>\frac{1}{2}E_{FS}$ [31,32]. The remaining loss mechanism is radiative escape (RE) in which the excited molecule decays into a discrete level of the lower electronic states and leaves the MOT, or decays back into the vibrational continuum in which case it escapes if each of the pair of atoms has a kinetic energy in excess of the trap well depth.

Using Eq. (22), we express the fraction of retained (nonescaping) atoms as

$$\mathcal{F}_{v'}\equiv\frac{1}{A_{v'}}\int_0^{2E_T}d\epsilon''A_{v'}(\epsilon''). \tag{25}$$

The value of $\mathcal{F}_{v'}$ as a function of the trap depth is shown in Fig. 9 for the $v'=88$ ^{7}Li singlet transition. $\mathcal{F}_{v'}$ increases with E_T oscillating gently due to contructive and destructive interference between the wave functions as the energy grows. Its magnitude depends on the level v'; the deeper the level the more it decays into the discrete vibrational levels [21]. Between E_T of 0.2 K and 1.0 K, $\mathcal{F}_{v'}$ varies approximately as E_T.

In Figs. 10 and 11, we show $\mathcal{F}_{v'}$ for the singlet and triplet transitions, respectively, of both isotopes, estimated using expression (25). We selected levels for which the fluorescence intensity signals should be the most reliable. They are $v'=62$ to 79 for ^{6}Li and 64 to 82 for ^{7}Li for singlet transitions [26], and $v'=56$ to 63 for ^{6}Li and 63 to 72 for ^{7}Li for triplet transitions [33]. The same general features are apparent with $\mathcal{F}_{v'}$ increasing with the trap depth and with v', and oscillations occurring due to overlapping wave functions. The general increase with v' does not hold for the lower levels. The curves may cross depending on E_T. The behavior can be traced back to the oscillation in the fraction of decays into the discrete vibrational levels of the ground

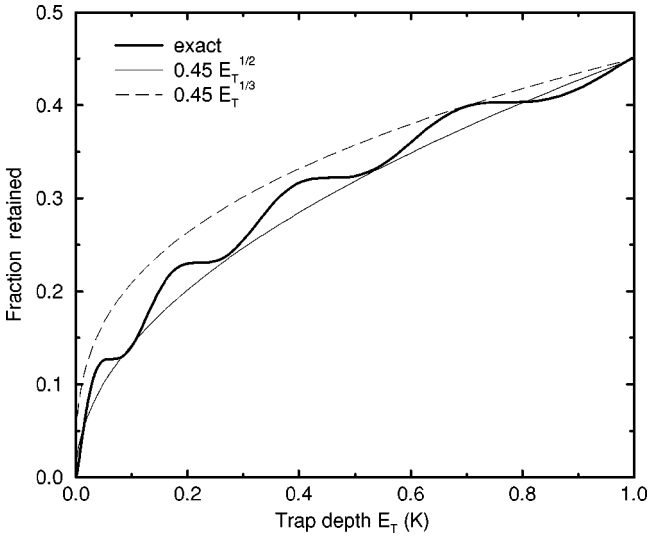

FIG. 9. Fraction of retained atoms $\mathcal{F}_{v'}$ for the excited singlet level $v'_S=88$ of $^7Li_2$ as a function of the trap depth E_T. The bold solid line represents the exact numerical result, and the thin solid line and the dashed line represent different power-law fits to the exact curve, respectively a square root and a cubic root dependence on E_T.

states [21] and the overlap with the continuum wave function; for lower v', the nodal structure of the ground-state wave functions, both continuum and discrete, becomes important. The fraction of atoms escaping from a trap with $E_T=1$ K is large, ranging from 0.97 to 0.68 and RE trap loss is important, even for deep traps.

Trap loss reduces the initial density n_0 of atoms. The corresponding diminution in the fluorescence intensity is proportional to the drop in the number of atom pairs undergoing photoabsorption and we can write for the decrease in the fluorescence intensity signal

$$I_F(v')\propto n_0(1-\mathcal{F}_{v'})\kappa_{v'}, \tag{26}$$

where $\kappa_{v'}(\nu,T)$ is the free-bound absorption rate per pair of atoms. The density of atoms escaping from the trap after spontaneous emission is $n=n_0[1-\mathcal{F}_{v'}(E_T)]$. In order to correct the values of $\kappa_{v'}$ for escape, we must first estimate the trap depth. $\mathcal{F}_{v'}(E_T)$ is highly dependent on both v' and E_T.

The MOT employed by Ritchie *et al.* [32] is anisotropic with the energy required to escape in one direction four times less than the energy required in an orthogonal direction. The trap depth can be varied and in the experiment the depth $E_T^{\min}$ of the shallowest point varied from 0.24 K to 0.38 K. Assuming an ellipsoidal geometry, we obtain for the average trap depth

$$E_T=\frac{1}{4\pi}\int d\Omega E_T(\theta,\phi)\simeq 2.8E_T^{\min}. \tag{27}$$

Thus 0.67 K$\leqslant E_T\leqslant$1.06 K. A more elaborate discussion on the trap depth can be found in Ritchie *et al.* [34].

The photoabsorption line strengths corrected for three different trap depths, 0.63 K, 1.00 K, and 1.25 K, are shown

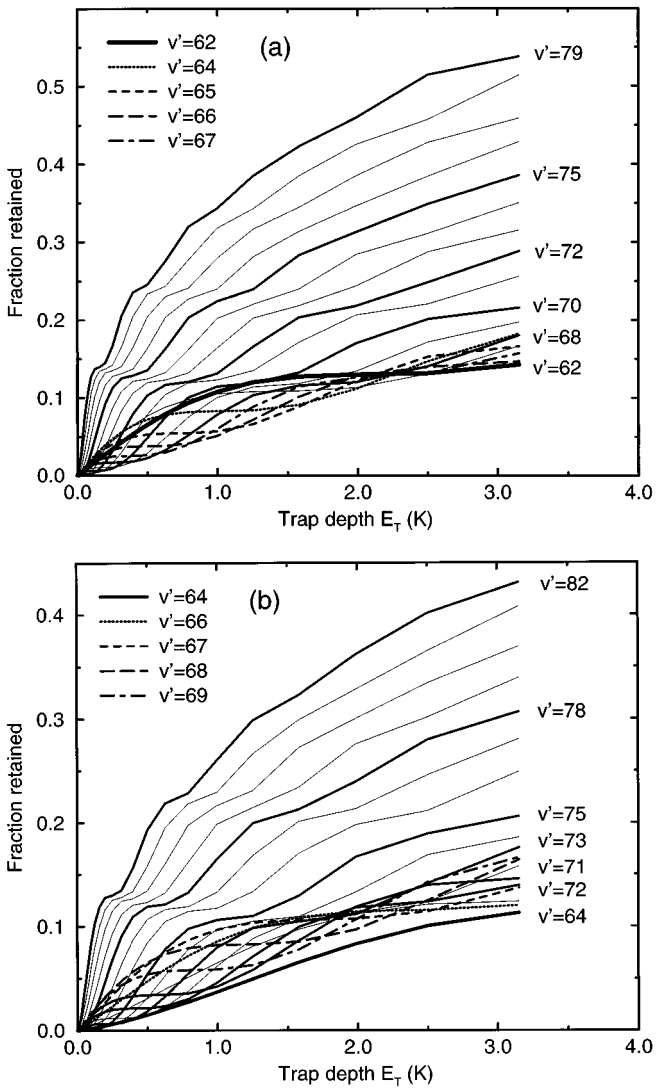

FIG. 10. $\mathcal{F}_{v'}$ for singlet vibrational levels (a) $v'=62-79$ of $^6Li_2$ and (b) $v'=64-82$ of $^7Li_2$ as a function of the trap depth E_T. The curves for the lower levels, identified by various line types, cross each other in contrast to the higher levels, which are well separated.

in Figs. 12(a) and 12(b) for the singlet transitions of ^{6}Li and ^{7}Li and in Figs. 13(a) and 13(b) for the triplet transitions.

The experimental values for the singlet transitions and the theoretical values are in qualitative agreement. The corrections for the partial retention of atoms following photoassociation and spontaneous emission affect some levels more than others, but with the probable uncertainty of the fluorescence signal of about 30% [33], all the corrected values fit within the error bars. For the singlet signals shown in Fig. 12, the influence of the corrections is stronger for local maxima situated around $v'_S\sim 67$ for ^{6}Li and $v'_S\sim 69$ for ^{7}Li and could yield the trap depth if measurement were more accurate. Although in principle the retained atoms could affect the determination of the scattering lengths from photoassociation spectra [26,22], the partial retention of atoms has no influence on the location of the minima since $\kappa_{v'}\sim 0$ for these levels. In the case of the triplet signals shown in Fig.

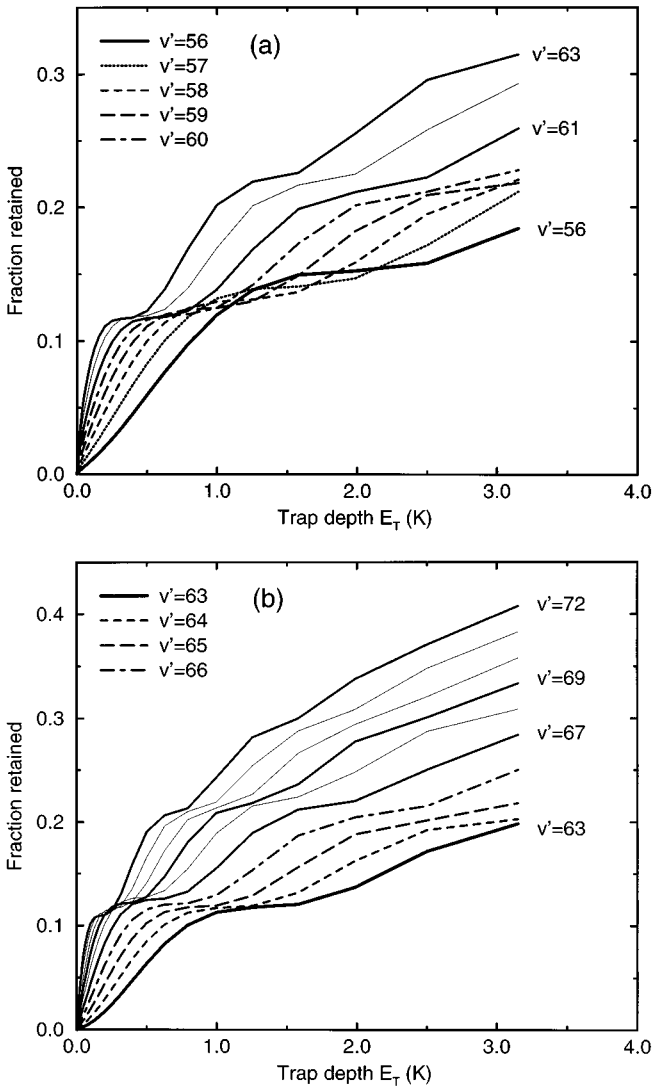

FIG. 11. $\mathcal{F}_{v'}$ for triplet vibrational levels (a) $v'=56-63$ of $^6Li_2$ and (b) $v'=63-72$ of $^7Li_2$ as a function of the trap depth E_T.

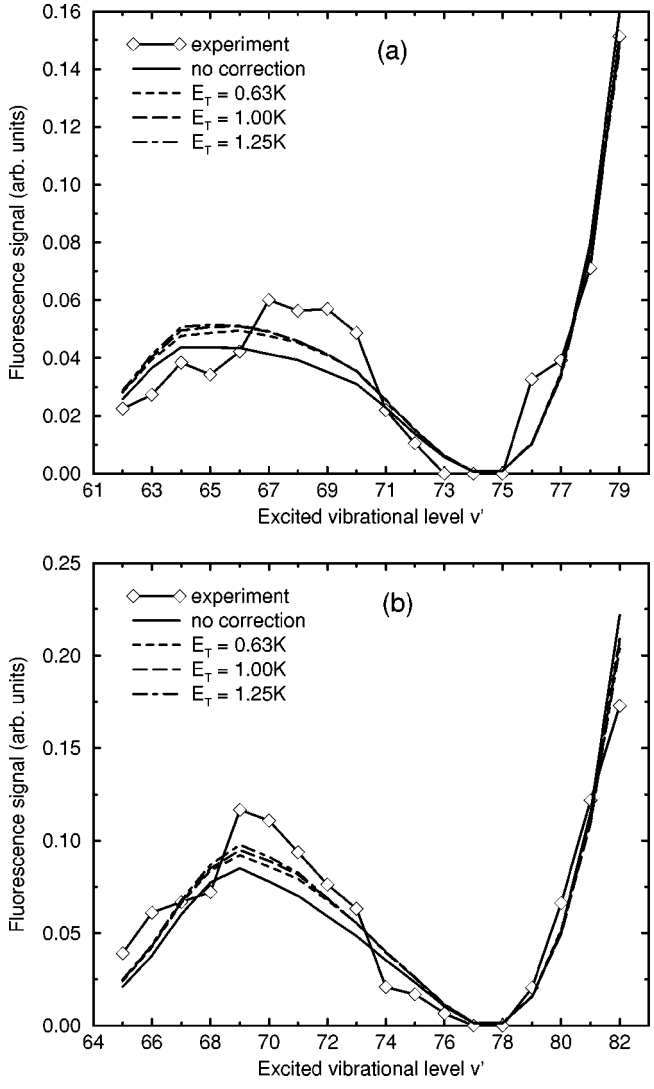

FIG. 12. Photoabsorption spectra at $T=1$ mK for singlet transitions. The experimental spectrum is compared with the theoretical values (no correction) and with values corrected for the trap loss, for three different trap depths: 0.63 K, 1.00 K, and 1.25 K. ^{6}Li is shown in (a) and ^{7}Li in (b).

13, the experimental values tend to level off at high v', contrary to the increase of the theoretical values. However, the influence of the trap depth is small and all the values fit within the experimental error bars. Greater accuracy is required before a reliable estimate of trap depth can be derived from the relative fluorescence measurements.

VI. QUADRATIC TRAP LOSS RATE

The efficiency of trap loss by radiative excitation in ^{7}Li gas has been measured by Kawanaka *et al.* [31] and Ritchie *et al.* [32] for photons slightly detuned from the atomic resonance frequency [35] and theoretical calculations have been carried out by Julienne and Vigué [36] and Julienne *et al.* [37]. The initial absorption occurs into a distribution of overlapping high lying vibrational levels. From our calculations, we can readily estimate the loss rate from radiative excitation following absorption into specific lower lying vibrational levels in the regime where the trap loss rate is proportional to the laser intensity and saturation has not occurred. The corresponding loss rate by radiative escape is equal to the absorption rate per photon $\kappa_{v'}$ times the flux φ of photons times the probability of escaping the trap. Thus

$$\beta_{\mathrm{RE}}(v')=2(1-\mathcal{F}_{v'})\kappa_{v'}\varphi, \tag{28}$$

where the factor of 2 arises because a pair of atoms escapes. In the photoassociative experiments of [9], the laser intensity I is 100 W/cm^2 and $\hbar\omega_p=445\,651.73$ GHz. For small detunings, the flux is related to I by $\varphi=I/h\nu\simeq I/\hbar\omega_p=3.38\times10^{20}$ photons cm^{-2} s^{-1}. In Table IV, we give $\beta_{\mathrm{RE}}(v')$ for the levels between -20 and -60 GHz and a trap depth $E_T=1$ K, where $\kappa_{v'}$ is evaluated for photoassociation at 1 mK. The quadratic trap loss varies between 10^{-14} and 10^{-12} cm^3/s. The values for ^{6}Li are larger because of the large negative scattering length. The values of β happen to be of the same order of magnitude as those measured at smaller detunings, namely 3×10^{-13} cm^3/s by Kawanaka *et al.* [31] and between 3×10^{-13} and 3×10^{-12} cm^3/s by Ritchie *et al.* [32].

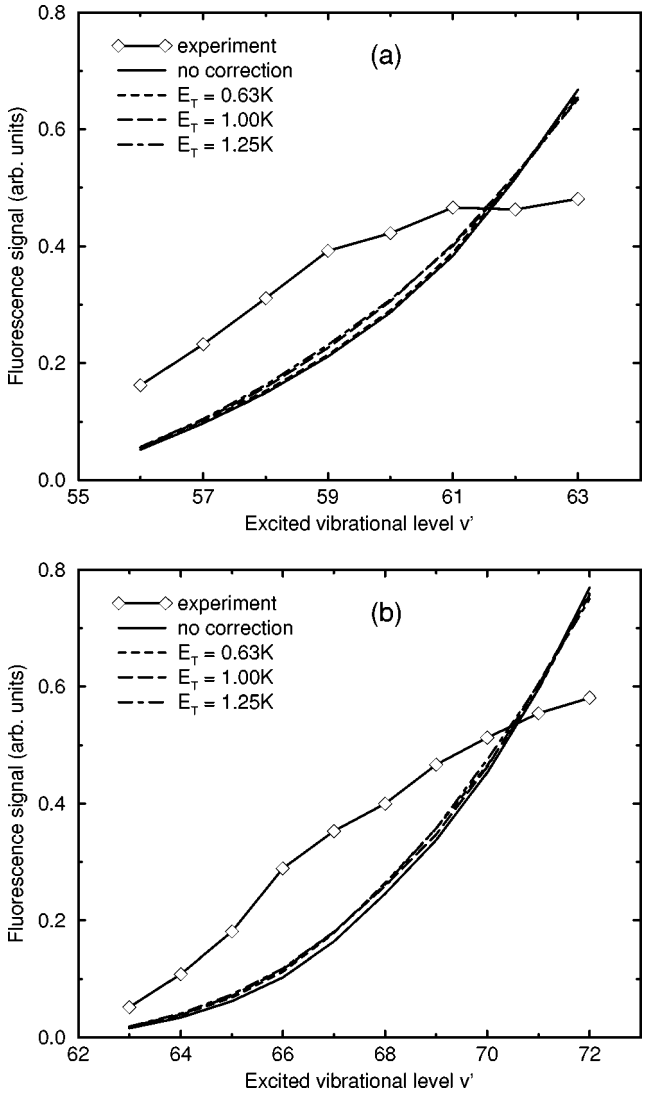

FIG. 13. As Fig. 11 for the triplet transitions with (a) for ^{6}Li and (b) for ^{7}Li.

TABLE IV. Quadratic trap loss rate coefficient β for the highest levels with Δ between 20 and 60 GHz and a trap depth $E_T=1$ K. The values for $\kappa_{v'}$ are given for $T=1$ mK. Brackets represent powers of ten.

v'	$\Delta_{v'}$ (GHz)	$\kappa_{v'}$ (cm^5)	$\mathcal{F}_{v'}$	β (cm^3/s)
		^{7}Li triplet		
86	26.116	2.10 [−33]	0.69	4.40 [−13]
85	35.219	1.61 [−33]	0.66	3.70 [−13]
84	46.469	1.24 [−33]	0.64	2.82 [−13]
83	60.202	9.70 [−34]	0.57	2.82 [−13]
		^{7}Li singlet		
95	22.005	1.15 [−33]	0.70	2.34 [−13]
94	29.835	8.00 [−34]	0.66	1.84 [−13]
93	39.868	5.60 [−34]	0.66	1.29 [−13]
92	51.758	3.94 [−34]	0.58	1.20 [−13]
		^{6}Li triplet		
80	22.608	1.14 [−32]	0.73	2.08 [−12]
79	31.580	9.41 [−33]	0.67	2.10 [−12]
78	42.989	7.86 [−33]	0.65	1.86 [−12]
77	57.097	6.61 [−33]	0.59	1.83 [−12]
		^{6}Li singlet		
88	21.407	1.04 [−33]	0.73	1.90 [−13]
87	29.809	6.81 [−34]	0.70	1.38 [−13]
86	40.470	4.45 [−34]	0.63	1.11 [−13]
85	53.874	2.90 [−34]	0.58	8.24 [−14]

VII. CONCLUSION

We have presented a theory of the photoassociation spectroscopy that relates the absorption line strengths to the properties of the free wave functions for the lowest singlet and triplet states of ^{6}Li and ^{7}Li isotopes. A direct link between the intensities and the scattering length is established.

We have studied spontaneous emission out of the excited molecular bound levels leading to radiative escape trap loss, showing that RE changes the density of atoms remaining in the trap. RE varies both with the trap depth E_T and the excited vibrational level v'. The fraction of atoms escaping the trap of 1 K depth after radiative decay from the excited level is substantial.

From a comparison of the experimental spectra with the theoretical predictions, estimates of the scattering length can be made [26,22]. In the case of the singlet transitions, for which the scattering lengths are positive for both ^{6}Li and ^{7}Li, the location of the first minimum in the fluorescence spectra as the detuning is increased yields the value of the scattering length. The retention of atoms has no influence on its location and previous results for a [26,22] are not affected. On the other hand, the location of the first local maximum yields in principle the trap depth. However, the accuracy of the measurements does not permit a definite estimate of its value. In the case of the triplet transitions, the spectra are monotonic, indicating a negative scattering length, and no useful estimate of the trap depth is possible.

ACKNOWLEDGMENTS

The authors are grateful to R. G. Hulet for useful discussions, and for making available the unpublished experimental data contained in Fig. 13. A.D. acknowledges the support of the Division of Chemical Sciences, Office of Basic Energy Sciences, U.S. Department of Energy. R.C. is supported by the National Science Foundation through the Institute for Theoretical Atomic and Molecular Physics (ITAMP). The presentation has been much improved through comments made by the W. C. Stwalley.

[1] J. Opt. Soc. Am. B **6**, 11 (1989), special issue on laser cooling and trapping of atoms, edited by S. Chu and C. Wieman.
[2] Laser Phys. **4** (1994), special issue on laser cooling and trapping, edited by V. Bagnanto, N. Bigelow, A. Dykhne, J. Weiner, and Y. Yakovlev.
[3] M. H. Anderson, J. R. Ensher, M. R. Matthews, C. E. Wieman, and E. A. Cornell, Science **269**, 198 (1995).
[4] C. C. Bradley, C. A. Sackett, J. J. Tollett, and R. G. Hulet, Phys. Rev. Lett. **75**, 1687 (1995).
[5] K. B. Davis, M.-O. Mewes, M. R. Andrews, N. J. van Druten, D. S. Durfee, D. M. Kurn, and W. Ketterle, Phys. Rev. Lett. **75**, 3969 (1995).
[6] J. D. Miller, R. A. Cline, and D. J. Heinzen, Phys. Rev. Lett. **71**, 2204 (1993); R. A. Cline, J. D. Miller, and D. J. Heinzen, *ibid.* **73**, 632 (1994).
[7] H. R. Thorsheim, J. Weiner, and P. S. Julienne, Phys. Rev. Lett. **58**, 2420 (1987).
[8] P. D. Lett, K. Helmerson, W. D. Phillips, L. P. Ratcliff, S. L. Rolston, and M. E. Wagshul, Phys. Rev. Lett. **71**, 2200 (1993).
[9] E. R. I. Abraham, N. W. M. Ritchie, W. I. McAlexander, and R. G. Hulet, J. Chem. Phys. **103**, 7773 (1995).
[10] R. Napolitano, J. Weiner, C. J. Williams, and P. S. Julienne, Phys. Rev. Lett. **73**, 1352 (1994).
[11] K. M. Sando and A. Dalgarno, Mol. Phys. **20**, 103 (1971).
[12] Joseph Noël Robin Côté, Ph.D. thesis, MIT, February (1995).
[13] R. Côté, A. Dalgarno, and M. J. Jamieson, Phys. Rev. A **50**, 399 (1994).
[14] W. T. Zembe and W. C. Stwalley, J. Phys. Chem. **97**, 2053 (1993).
[15] C. Linton, F. Martin, I. Russier, A. J. Ross, P. Crozet, S. Churassy, and R. Bacis, J. Mol. Spectrosc. **175**, 340 (1996).
[16] P. Kusch and M. M. Hessel, J. Chem. Phys. **67**, 586 (1977).
[17] I. Schmidt-Mink, W. Müller, and W. Meyer, Chem. Phys. **94**, 263 (1985).
[18] C. Linton, T. L. Murphy, F. Martin, R. Bacis, and J. Verges, J. Chem. Phys. **91**, 6036 (1989).
[19] M. Marinescu and A. Dalgarno, Phys. Rev. A **52**, 311 (1995).
[20] Z.-C. Yan, J. F. Babb, A. Dalgarno, and G. W. F. Drake, Phys. Rev. A **54**, 2824 (1996).
[21] R. Côté and A. Dalgarno, Chem. Phys. Lett. **279**, 50 (1997).
[22] E. R. I. Abraham, W. I. McAlexander, J. M. Gerton, R. G. Hulet, R. Côté, and A. Dalgarno, Phys. Rev. A **55**, R3299 (1997).
[23] K. Urbansky, S. Antonova, A. Yiannopoulos, A. M. Lyyra, Li Li, and W. C. Stwalley, J. Chem. Phys. **104**, 2813 (1996).
[24] L. B. Ratcliff, J. L. Fish, and D. D. Konowalow, J. Mol. Spectrosc. **122**, 293 (1987).
[25] P. Pillet, A. Crubellier, A. Bleton, O. Dulieu, P. Nosbaum, I. Mourachko, and F. Masnou-Seeuws, J. Phys. B **30**, 2801 (1997).
[26] E. R. I. Abraham, W. I. McAlexander, J. M. Gerton, R. G. Hulet, R. Côté, and A. Dalgarno, Phys. Rev. A **53**, R3713 (1996).
[27] R. Côté, A. Dalgarno, Y. Sun, and R. G. Hulet, Phys. Rev. Lett. **74**, 3581 (1995).
[28] E. R. I. Abraham, W. I. McAlexander, C. A. Sackett, and R. G. Hulet, Phys. Rev. Lett. **74**, 1315 (1995).
[29] W. I. McAlexander, E. R. I. Abraham, and R. G. Hulet, Phys. Rev. A **54**, R5 (1996); See also Z. Lin, K. Shimizu, M. Zhan, F. Shimizu, and H. Takuma, Jpn. J. Appl. Phys., Part 1 **30**, 1324 (1991).
[30] See the review by P. S. Julienne, A. M. Smith, and K. Burnett, in *Advances in Atomic, Molecular, and Optical Physics*, edited by D. R. Bates and B. Bederson (Academic, San Diego, 1993), Vol. 30, p. 141.
[31] J. Kawanaka, K. Shimizu, H. Takuma, and F. Shimizu, Phys. Rev. A **48**, R883 (1993).
[32] N. W. M. Ritchie, E. R. I. Abraham, Y. Y. Xiao, C. C. Bradley, and R. G. Hulet, Phys. Rev. A **51**, R890 (1995).
[33] R. G. Hulet (private communication).
[34] N. W. M. Ritchie, E. R. I. Abraham, and R. G. Hulet, Laser Phys. **4**, 1066 (1994).
[35] The experimental detunings were -8 MHz for Kawanaka *et al.* [31] and -2.3Γ, -2.9Γ, -3.5Γ, and -4.1Γ ($\Gamma = 5.8$ MHz) for Ritchie *et al.* [32].
[36] P. S. Julienne and J. Vigué, Phys. Rev. A **44**, 4494 (1991).
[37] P. S. Julienne, C. Williams, O. Dulieu, and Y. B. Band, Laser Phys. **4**, 1076 (1994).